Deregularization of a smooth system – example hydraulics

Friedrich Pfeiffer

Abstract Many technical systems include steep characteristics for force laws, which as a rule lead to stiff differential equations and large computing times. For the dynamical performance such steep characteristics are very near to laws with set-valued properties and might therefore be replaced by set-valued force laws. This is true for multibody dynamics including unilateral contacts, and it is in an approximate way true for fluid mechanical systems like hydraulics. In the following we present a new modeling scheme for hydraulic systems, which establishes the hydraulic equations of motion in the form of multibody system eqations with bilateral and unilateral constraints, and which is able to reduce computing times by three to four order of magnitudes. A large industrial example illustrates the excellent performance of the new theory.

Keywords Deregularization of smooth systems ·
Complementarities · System models · Hydraulics

1. Introduction

Models approximate the physical or technical reality. They are more or less detailed, but all models include

F. Pfeiffer
Institute of Applied Mechanics, Technical University
Munich, Boltzmannstrasse 15, D-85748 Garching,
Germany
e-mail: pfeiffer@amm.mw.tum.de

some degree od approximation. The real world cannot be modeled in a perfect way. Therefore, in establishing models we should keep in mind, that technical systems and especially technical mechanics are not deductive systems. This is true for classical analytical mechanics, which applies only partly to problems of some realistic significance. A further aspect concerns the goals connected with models. Do we want to map reality as perfect as possible, or do we want to consider certain parameter influences? Both objectives include difficult problems, because a model is by itself dumb. We have to make a model intelligent by introducing into it our knowledge of the problem under consideration, the physical and technical properties as good as we understand them, the parameter influences as good as we might expect them, the neglections as good as we can estimate them. This all is more an art than a science, but it is so essential, that no good model can be established without a preliminary phase of physical, of mechanical argueing leading to a sound imagination and a sound picture of the real world problem to be modeled.

Simple models for the evaluation of tendencies with respect to the performance of a system include some really difficult problems, because such simple models not only afford a perfect view of the overall system but also a perfect idea of what is important and of what is not important. In addition simple system modeling might be faulty, because the interference of many degrees of freedom might result in a completely different dynamical behavior as compared with simple considerations.

A recently published finding with respect to the well known friction problem of self-excited oscillations connected with falling characteristics illustrates especially this danger of coming out with incorrect results. Including more than one degree of freedom it can be shown, that self-excited oscillations may happen also for an increasing and not for a falling characteristic [2].

After having dealt with this model finding phase, which by the way is usually very much underestimated, we must find a decision on the mathematical and especially on the numerical tools we want to apply. For one and the same problem we have a variety of possible mathematical descriptions with again a certain variety of numerical algorithms. Some usual criteria for this choice are physical-mathematical correspondence, structural features of the resulting equations, transformation capabilities with the goal of analytical or partly analytical solutions, convergence of the solutions, stability of the numerical algorithms and finally the representation of the results allowing clear interpretations.

Coming back to our problem of descibing systems with force laws including very steep characteristics we may apply two approaches, a smooth and a nonsmooth one. In practical engineering characteristics with steep features occur in connection with contact problems, with fluidmechanical problems of hydraulic equipment, with cavitation or with electronic switching problems, to name only a few examples. From the mathematical and from the resulting numerical standpoint of view such characteristics produce either stiff differential equations or they require a complementarity formulation. The decision which way to go depends mainly on the computation time.

Considering contacts and related problems we might discretize a contact by evaluating the local stiffness properties of the contact, which allows the derivation of a force law. As contact stiffnesses are usually very large, we come out with stiff differential equations. The second way consists in assuming the local contact area as rigid, which does not imply that the whole body must be assumed rigid, and to formulate the contact properties by complementarities [7, 8]. In hydraulic networks we find such a complementarity behavior in connection with check valves, with servo valves and with cavitation in fluid-air-mixtures. For example a check valve might be open, then we have approximately no pressure drop, but a certain amount of the flow rate. Or a check valve might be closed, then we have a pressure drop, but no flow rate. A small amount of air in the fluid will be compressed by a large pressure to a neglectable small air volume, but for a very small pressure the air will expand in a nearly explosive way, a behavior, which can be approximated by a complementarity [1, 9].

The area of non-smooth mechanics has been established during the last thirty years by Moreau in Montpellier and by Panagiotopoulos in Thessaloniki [6]. During the nineties these theories have been transfered and applied to multibody system dynamics [7, 8] and since then furtheron developed in a very concise and rigorous way [4, 5]. The research with respect to numerical methods is still on the way, because efficient numerical methods are the key for applications with respect to large technical systems [3]. The paper will be mainly based on findings of the dissertation [1] and some publication [9]. Therefore the description of the new hydraulic theory will be kept short.

2. Modeling hydraulics

In order to set up a mathematical model we assume, that the hydraulic system can be considered as a network of basic components. These components are connected by nodes. In conventional simulation programmes these nodes are assumed to be elastic. In the case of relatively large volumes this assumption is reasonable whereas for very small volumes incompressible junctions, with unilateral or bilateral behavior, are a better approach. Complex components like control valves can be composed of elementary components like lines, check valves and so forth. In the following a selection of elementary components is considered. It is shown how the equations of motion are derived and how they are put together to form a network.

2.1. Junctions

Junctions are hydraulic volumes filled with oil. The volumes may be considered as constant volumes or variable volumes as shown in Fig. 1. Junctions with variable volume are commonly used for hydraulic cylinders.

2.1.1. Compressible junctions

Assuming compressible fluid in such a volume leads to a nonlinear differential equation for the pressure p.

Fig. 1 Hydraulic junctions with constant and variable volume
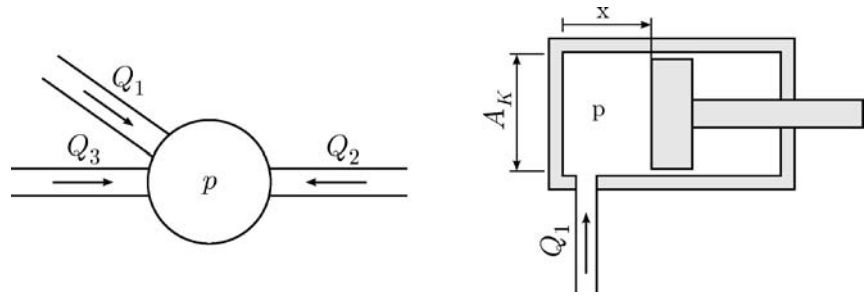
Introducing the pressure-dependent bulk modulus

$$E(p) = -V \frac{dp}{dV} \qquad (1)$$

yields a differential equation for the pressure in a constant volume

$$\dot{p} = \frac{E}{V} \sum Q_i \qquad (2)$$

and

$$\dot{p} = \frac{E}{V} (Q_1 - A_K \dot{x}) \qquad (3)$$

in a variable volume, respectively. A common assumption with respect to the fluid properties considers a mixture of linear elastic fluid with a low fraction of air. Fig. 2 shows the calculated specific volume of a mixture of oil and 1% air (at a reference value of 1 bar). For high pressure values the air is compressed to a neglectable small volume whereas the air expands abruptly for low pressure values, see Fig. 2 with the pressure p versus the specific volume v. This figure illustrates also that the curve for the pressure in dependency of the specific

volume can be very well approximated by a unilateral characteristic. If we would choose a smooth model we would get stiff differential Equations (2) and (3) for very small volumes $V \to 0$.

2.1.2. Incompressible junctions

To avoid stiff differential equations for small volumes it is obviously possible to substitute the differential equations by algebraic equations. Assuming a constant specific volume of the incompressible fluid yields for a constant and a variable volume, respectively, the following algebraic equations:

$$\sum Q_i = 0 \quad \text{respectively} \quad \sum Q_i - A_K \dot{x}_K = 0 \quad (4)$$

These equations consider neither the elasticity nor the unilaterality of the fluid properties. A fluid model covering both elasticity and unilaterality is described in Section 2.1.1. In the case of neglectable small volumes the fluid properties can be approximated by a unilateral characteristic. As illustrated in Fig. 2 a unilateral law

Fig. 2 Fluid expansion for low pressures
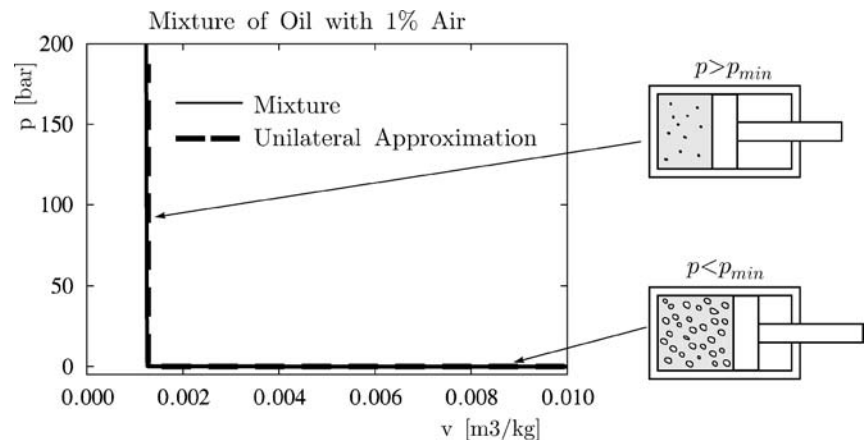
can be established by introducing a state variable

$$\bar{V} = -\int_0^t \sum Q \, d\tau \tag{5}$$

which represents the total void volume in a fluid volume. Obviously this void volume is restricted to be positive, $\bar{V} \geq 0$. As long as the pressure value is higher than a certain minimum value $p_{\min}$, the void volume is zero.

A void formation starts when the pressure p approaches the minimum value $p_{\min}$. This idealized fluid behavior can be described by a so called corner law or Signorini's law [7].

$$\bar{V} \geq 0; \quad \bar{p} \geq 0; \quad \bar{V} \cdot \bar{p} = 0 \tag{6}$$

The pressure reserve $\bar{p}$ is defined by $\bar{p} = p - p_{\min}$. By differentiation the complementarity can be put on a velocity level.

$$\dot{\bar{V}} = \sum Q_i \geq 0 \,, \tag{7}$$

The equality sign represents the Kirchhoff equation stating that the sum of all flow rates into a volume is equal to the sum of all flow rates out of the volume. If the outflow is higher than the inflow the void volume increases, $\dot{\bar{V}} > 0$. Substituting the flow rates Q into a fluid volume by the vector of the velocities in the connected lines and the corresponding areas,

$$\boldsymbol{v} = \begin{bmatrix} v_1 \\ v_2 \\ \vdots \\ v_i \end{bmatrix} \qquad \boldsymbol{W} = \begin{bmatrix} A_1 \\ A_2 \\ \vdots \\ A_i \end{bmatrix} \tag{8}$$

yields the junction equation in the unilateral form

$$-\boldsymbol{W}^T \boldsymbol{v} \geq 0 \,. \tag{9}$$

It is evident that fluid volumes with non-constant volume can be put also into this form by extending the velocity and area vectors by the velocity and the area of the piston, respectively. As long as the pressure is higher than the minimum value, $\bar{p} > 0$, the unilateral Equation (9) can be substituted by a bilateral equation $\boldsymbol{W}^T \boldsymbol{v} = 0$. In this case it is necessary to verify the

validity of the assumption $\bar{p} > 0$ because the bilateral constraint does not prevent negative values of $\bar{p}$.

2.2. Valves

In the following we shall give some examples of modelling elementary valves and more complex valves as a network of basic components. Physically, any valve is a kind of controllable constraint, whether the working element be a flapper, ball, needle etc.

2.2.1. Orifices

Orifices with variable areas are used to control the flow in hydraulic systems by changing the orifice area. As illustrated in Fig. 3 the pressure drop in an orifice shows a nonlinear behavior. The classical model to calculate the pressure drop Δp in dependency of the area A_V and the flow rate Q is the Bernoulli equation.

$$\Delta p = \frac{\rho}{2} \left(\frac{1}{\alpha A_V} \right)^2 Q |Q| \tag{10}$$

The factor α is an empirical magnitude considering geometry- and Reynoldsnumber-depending pressure losses. It must be determined experimentally.

As long as the valve is open the pressure drop can be calculated as a function of flow rate and the valve area, Equation (10). As shown in Fig. 3 the characteristic becomes infinitely steep when the valve closes. In most commercial simulation programmes this leads to numerical ill-posedness and stiff differential equations for very small areas. In order to avoid such numerical problems the characteristic for the pressure drop of closed valves can be replaced by a simple constraint
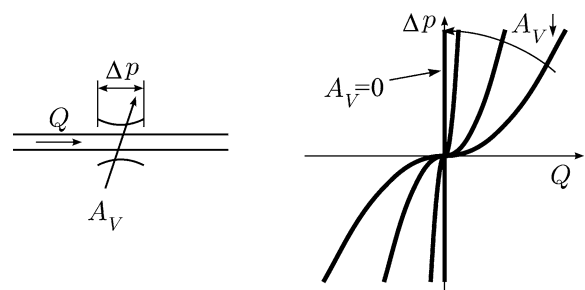

Fig. 3 Pressure drop in an orifice

equation.

$$Q = Av = 0 \quad \text{respectively} \quad A\dot{v} = 0 \qquad (11)$$

This constraint has to be added to the system equations when the valve closes. In the case of valve opening it has to be removed again. This leads to a time-varying set of constraint equations. In order to solve the system equations one has to distinguish between active constraints (closed valves) and passive constraints (opened valves). The last ones can be removed. The constraint equations avoid stiff differential equations. On the other hand they require to define active and passive sets [4, 7, 8].

2.2.2. Check valves

Check valves are directional valves that allow flow in one direction only. It is not worth trying to describe all existing types, so only the basic principle and the mathematical formulation is presented.

Figure 4 shows the principle of a check valve with a ball as working element. Assuming lossless flow in one direction and no flow in the other direction results in two possible states:

- Valve open: pressure drop $\Delta p = 0$ for all flow rates $Q \geq 0$
- Valve closed: flow rate $Q = 0$ for all pressure drops $\Delta p \geq 0$

Again these two states can be described by a corner law

$$Q \geq 0; \quad \Delta p \geq 0; \quad Q \cdot \Delta p = 0. \qquad (12)$$

Prestressed check valves with springs show a modified unilateral behavior, see Fig. 5.

The pressure drop curve of a prestressed check valve can be split into an ideal unilateral part Δp_1 and a
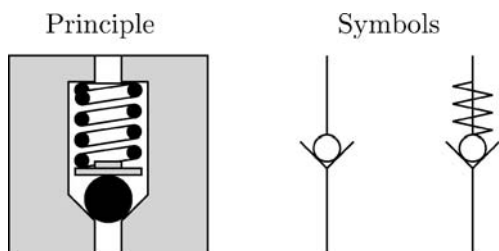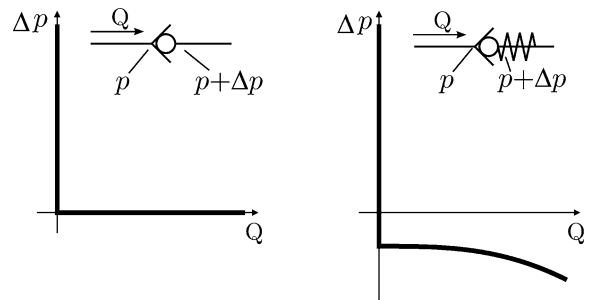
Fig. 5 Check valve characteristics

smooth curve Δp_2 considering the spring tension and pressure losses, see Fig. 6

2.2.3. Combined components

Many hydraulic standard components are combinations of basic elements. Since the combination of unilateral and smooth characteristics yields either non-smooth or smooth behavior it is worth to consider such components with a smooth characteristic separately. As an example we consider a typical combination of a throttle and a check valve. Figure 7 shows the symbol and the characteristics of both components. Since the flow rate of the combined component is the sum of the flows in the check valve and the throttle, the sum of the flow rates is a smooth curve. In such cases it is convenient to model the combined component as a smooth component (in the mechanical sense as a smooth force law).

2.2.4. Servovalves

As an example for a servovalve we consider a one-stage 4-way-valve. It is a good example for the complexity of the networks representing such components like valves, pressure control valves, flow control valves and related valve systems. Multistage valves can be modelled in
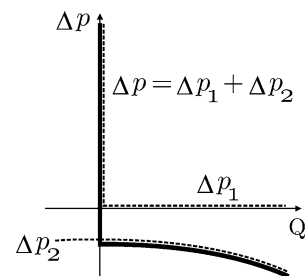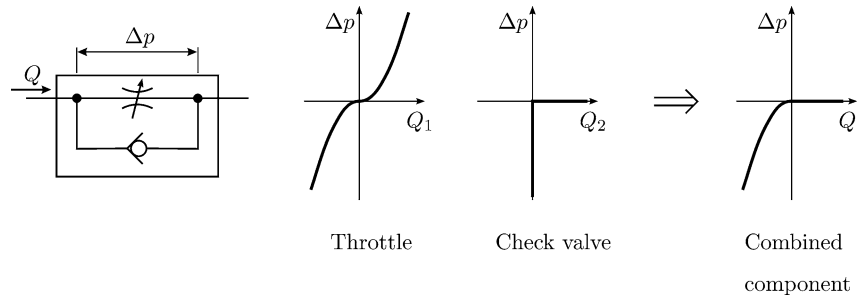
Fig. 4 Check valve

Fig. 6 Superposition of unilateral and smooth curves

Fig. 7 Combination of smooth and non-smooth components

Throttle   Check valve   Combined
                                                  component

a similar way as a network consisting of servovalves and pistons, which themselves are working elements of the higher stage valve. Figure 8 shows the working principle of a 4-way valve. Moving the control piston to the right connects the pressure inlet P with the output B and simultaneously the return T with the output A. If one connects the outputs A and B with a hydraulic cylinder, high forces can be produced with small forces

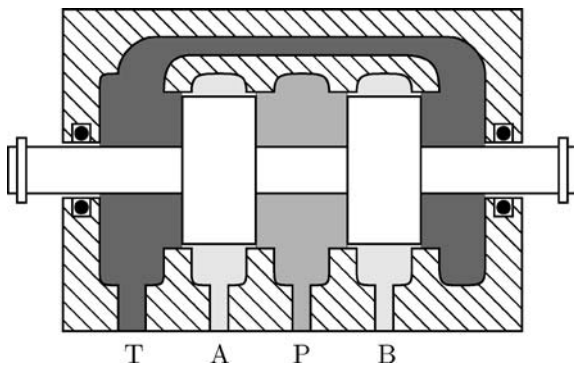acting on the control piston. The valve works like a hydraulic amplifier.

Figure 9 shows a network model of the 4-way valve. The areas of the orifices $A_{V1} \ldots A_{V4}$ are controlled by the position x of the piston. The orifice areas are assumed to be known functions of the position x. The parameter δ covers a potential deadband. To derive the equations of motion the lines in the network are assumed to be flow channels with cross sectional areas $A_1 \ldots A_4$. The fluid is incompressible since the volumes are usually very small, and the bulk modulus of the oil is very high. The oil masses in the lines are $m_1 \ldots m_4$. Denoting the junction pressures with p_i and the pressure drops in the orifices with Δp_i, we get the equations of momentum as

Fig. 8 4-way valve

$$m_1 \dot{v}_1 - A_1 p_1 + A_1 p_2 + A_1 \Delta p_1 = 0$$
$$m_2 \dot{v}_2 - A_2 p_2 + A_2 p_3 + A_2 \Delta p_2 = 0$$
$$m_3 \dot{v}_3 - A_3 p_3 + A_3 p_4 + A_3 \Delta p_3 = 0 \qquad (13)$$
$$m_4 \dot{v}_4 + A_4 p_1 - A_4 p_4 + A_4 \Delta p_4 = 0$$
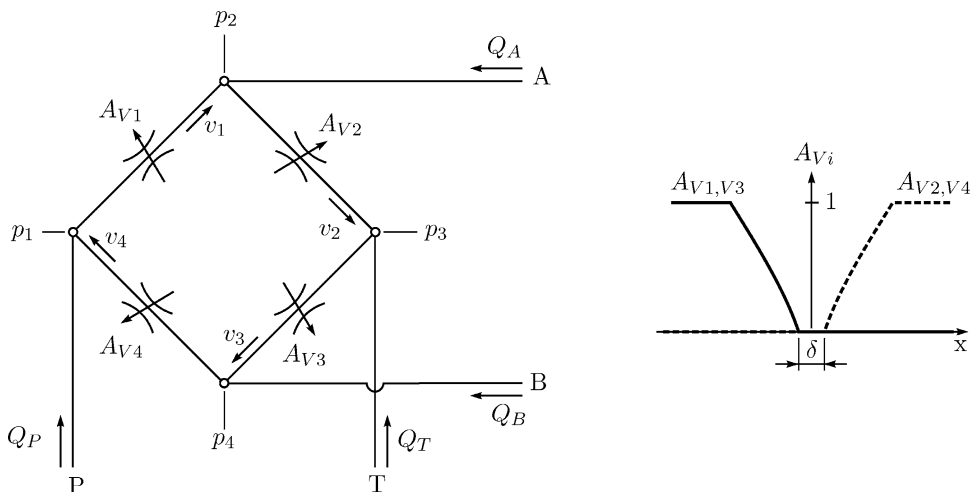
Fig. 9 Network model of a 4-way valve

which can be expressed as

$$\boldsymbol{M\dot{v}} + \boldsymbol{Wp} + \boldsymbol{W}_V\Delta\boldsymbol{p} = \boldsymbol{W}_a\Delta\boldsymbol{p}_a. \tag{14}$$

where $\boldsymbol{v}$ is the vector of flow velocities, $\boldsymbol{p}$ the vector of junction pressures, $\Delta\boldsymbol{p}$ the vector of pressure drops in the closed orifices and $\Delta\boldsymbol{p}_a$ the vector of pressure drops in the open orifices. The mass matrix $M = \mathrm{diag}(m_i)$ is the diagonal matrix of the oil masses. The matrix

$$\boldsymbol{W} = \begin{bmatrix} -A_1 & A_1 & 0 & 0 \\ 0 & -A_2 & A_2 & 0 \\ 0 & 0 & -A_3 & A_3 \\ A_4 & 0 & 0 & -A_4 \end{bmatrix}$$

is used to calculate the forces acting on the oil masses in the channels resulting from the junction pressures $\boldsymbol{p}$. The junction equations are given by

$$\begin{bmatrix} Q_P \\ Q_A \\ Q_T \\ Q_B \end{bmatrix} + \begin{bmatrix} -A_1 & 0 & 0 & A_4 \\ A_1 & -A_2 & 0 & 0 \\ 0 & A_2 & -A_3 & 0 \\ 0 & 0 & A_3 & -A_4 \end{bmatrix} \begin{bmatrix} v_1 \\ v_2 \\ v_3 \\ v_4 \end{bmatrix} = \boldsymbol{0} \tag{15}$$

which can be written in the form

$$\boldsymbol{Q}_{\mathrm{in}} + \boldsymbol{W}^T\boldsymbol{v} = \boldsymbol{0} \, . \tag{16}$$

In order to determine the pressure drops Δp_i one has to distinguish between open and closed orifices to avoid stiff equations, see Section 2.2.1. In case of open orifices the pressure drop can be calculated directly subject to the given flow rates and the orifice area, whereas closed orifices are characterized by a constraint equation.

$$\begin{aligned} \Delta p_{ai} &= f\,(v_i, A_{Vi}(x)) \text{ open orifices } i \\ A_j v_j &= 0 \qquad\qquad\quad \text{closed orifices } j \end{aligned} \tag{17}$$

The constraint equations for the closed orifices are collected to give

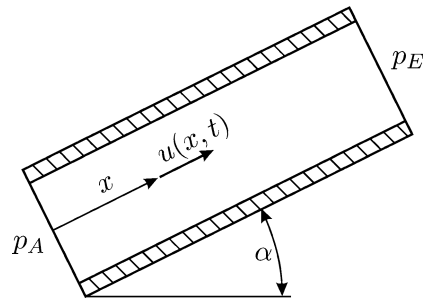$$\boldsymbol{W}_V^T\boldsymbol{v} = \boldsymbol{0} \tag{18}$$

Fig. 10 Coordinates for one-dimensional flow

where the number of columns of $\boldsymbol{W}_V$ is the number of closed orifices. Note that this matrix has to be updated every time an orifice opens or closes.

2.3. Hydraulic lines

Hydraulic lines or hoses are used to connect components. For long lines the dynamics of the compressible fluid has to be taken into account. In order to get a precise system model, it is necessary to investigate pressure wave phenomena as well as the pipe friction. The pipe friction is rather complicated since the velocity profile is not known a priory. In the case of laminar flow it is possible to derive analytical formulas for a uniform fluid transmission line in the Laplace domain. The so-called 4-pole-transfer-functions relate the pressure and the flow at the input and at the output of the line in dependency of Bessel functions. Many attempts have been made to approximate the transfer functions with rational polynomial functions which can be re-transformed into the time domain. Unfortunately the form of the equations of these models is not compatible with the equations in the framework of this paper, because the coupling with constraint equations might lead to numerical instability due to violation of the principle of virtual work.

In the following a time domain modal approximation is presented. This model can be extended to cover frequency dependent friction as well. The starting point are the linearized partial differential equations for one-dimensional flow. The coordinates are shown in Fig. 10. Partial derivatives of a arbitrary coordinate q are denoted by $\frac{\partial q}{\partial t} = \dot{q}$ and $\frac{\partial q}{\partial x} = q'$, respectively.

The mass balance

$$\dot{p} + \frac{E}{A}Q' = 0 \tag{19}$$

with the flow rate $Q = Au$ and the introduced state variable

$$\tilde{x} = \frac{1}{A} \int_0^t Q d\tau \; ; \quad \dot{\tilde{x}} = \frac{Q}{A} \; ; \quad \ddot{\tilde{x}} = \frac{\dot{Q}}{A} \tag{20}$$

can be solved analytically with respect to the pressure p:

$$p(x, t) = -\frac{E}{A} \int_0^t Q' d\tau + p_0(x)$$

$$= -E \int_0^t \dot{\tilde{x}}' d\tau + p_0(x) \tag{21}$$

respectively

$$p(x, t) = -E\tilde{x}' + p_0(x) \tag{22}$$

The term $p_0(x)$ represents the initial pressure distribution in the line. The equation of momentum

$$\rho \dot{u} + p' + f_R + f_g = 0 \tag{23}$$

with a friction force f_R and a gravity force f_g can be transformed with Equation (20) to

$$\rho \ddot{\tilde{x}} - E\tilde{x}'' + p_0' + f_R + f_g = 0 . \tag{24}$$

Multiplying Equation (24) with arbitrary test functions $w(x)$ and integrating over the length L of the line yields the weak formulation

$$\rho \int_0^L \ddot{\tilde{x}} w(x) dx - E \int_0^L \tilde{x}'' w(x) dx$$

$$+ \int_0^L p_0'(x) w(x) dx + \int_0^L f_R w(x) dx$$

$$+ \int_0^L f_g w(x) dx = 0 \quad \forall \, w(x) \tag{25}$$

where the term $w\tilde{x}''$ can be integrated by parts to fit the boundary conditions.

$$\int_0^L w\tilde{x}'' dx = w\tilde{x}'|_0^L - \int_0^L w'\tilde{x}' dx$$

$$= w_L \frac{1}{E}(p_0(L) - p_E)$$

$$- w_0 \frac{1}{E}(p_0(0) - p_A) - \int_0^L w'\tilde{x}' dx \tag{26}$$

p_A, p_E are boundary pressures and w_0, w_L are the values of the test function $w(x)$ at the boundaries ($x = 0$, $x = L$). For the sake of simplicity the initial pressure distribution is assumed to be uniform, $p_0(x) = p_0 = $ const. In order to approximate the partial differential equations by a set of ordinary differential equations we introduce spatial shape functions $w(x)$ and a separation of the variables x and t,

$$\tilde{x} \approx \boldsymbol{q}(t)^T \boldsymbol{w}(x) \tag{27}$$

According to Galerkin's method the shape functions $\boldsymbol{w}(x)$ are the same functions used in the weak formulation, Equation (25). The discretized equations of motion are then

$$\rho \int_0^L \boldsymbol{w}\boldsymbol{w}^T dx \ddot{\boldsymbol{q}} + E \int_0^L \boldsymbol{w}'\boldsymbol{w}'^T dx \boldsymbol{q} + \int_0^L f_R \boldsymbol{w} dx$$

$$+ \int_0^L f_g \boldsymbol{w} dx = w_0 p_A - w_L p_E - (w_0 - w_L) p_0 \tag{28}$$

which can be transformed with $\boldsymbol{w}_A = A\boldsymbol{w}_0$, $\boldsymbol{w}_E = A\boldsymbol{w}_L$ to

$$\boldsymbol{M}\ddot{\boldsymbol{q}} + \boldsymbol{K}\boldsymbol{q} + \boldsymbol{W}\boldsymbol{p} = -A \int_0^L f_R \boldsymbol{w} dx$$

$$- A \int_0^L f_g \boldsymbol{w} dx - (\boldsymbol{w}_A - \boldsymbol{w}_E) p_0 \tag{29}$$

with the abbreviations

$$M = \rho A \int_0^L w w^T x \quad \text{(mass matrix)}$$

$$K = E A \int_0^L w' w'^T \quad \text{(stiffness matrix)}$$

$$W = (-w_A \quad w_E) \quad .$$

Equation (29) is similar to the equations of motion of a mechanical system. Suitable functions $w(x)$ are harmonic functions and B-spline functions, as numerical experiments confirmed.

2.3.1. Frequency dependant friction

In case of laminar flow the cross-sectional velocity profile of oscillatory flow can be calculated analytically as functions of Bessel functions. It turns out that the gradient of the velocity becomes higher with increasing frequencies ω. Figure 11 shows calculated profiles for dimensionless frequencies $\frac{\omega}{\nu} R$ where R is the radius and ν the kinematic viscosity.

For low frequencies the profile is the well-known parabolic Hagen-Poiseuille profile for stationary flow. Since the friction force depends on the gradient at the pipe wall the friction force becomes higher with increasing frequency. Therefore the increasing friction has to be taken into account by a correction of the steady-state friction factor. It can be shown that the pipe friction for a parabolic velocity profile can be covered by a damping matrix D_0

$$M\ddot{q} + D_0 \dot{q} + K q = h \qquad (30)$$

with

$$D_0 = 8 \mu \pi \int_0^L w w^T dx. \qquad (31)$$

Since the parabolic velocity profile is valid only for low frequencies this damping matrix has to be corrected. In the Laplace domain a friction correction factor can be derived as

$$N = \frac{\frac{\partial U}{\partial r}\big|_R}{-\frac{4}{R}} = -\frac{R}{8} \gamma \left(\frac{J_{-1}(\gamma R) - J_1(\gamma R)}{J_2(\gamma R)} \right) \qquad (32)$$

where

$$\gamma = \sqrt{\frac{-\rho s}{\mu}} . \qquad (33)$$

With the dimensionless frequency $k_H = \sqrt{\frac{\omega}{\nu}} R$ the following approximation of the real part of Equation (32) can be given (see [1]):

$$N(k_H) = \begin{cases} 1 + 0.0024756 \cdot k_H{}^{3.0253322} & k_H \leq 5 \\ (N(5) - 0.175 \cdot 5) + 0.175 \cdot k_H & k_H > 5 \end{cases} \qquad (34)$$

In order to correct the damping matrix the eigenvalues λ_i and the eigenfrequencies

$$\omega_i = \sqrt{\lambda_i} \qquad (35)$$

of the matrix $M^{-1}K$ are calculated. The eigenvectors are collected in the orthogonal modal matrix

$$\Phi = (\Phi_1, \Phi_2, \ldots, \Phi_n) . \qquad (36)$$

$\sqrt{\frac{\omega}{\nu}} R = 1$ $\qquad\qquad$ $\sqrt{\frac{\omega}{\nu}} R = 10$ $\qquad\qquad$ $\sqrt{\frac{\omega}{\nu}} R = 100$

$u_n(r)$

Fig. 11 Normalized velocity profiles for oscillatory flow

With a diagonal correction matrix $\bar{N} = \text{diag}(N(\omega_i))$ a corrected modal damping matrix is introduced in the form

$$D_m = \Phi^T D_0 \Phi \cdot \bar{N} \tag{37}$$

which can be re-transformed to yield

$$D = (\Phi^T)^{-1} D_m \Phi^{-1} \tag{38}$$

With this matrix the friction term in Equation (29) can be substituted:

$$A \int_0^L f_R w \, dx = D\dot{q} \tag{39}$$

2.4. Hydraulic networks

Hydraulic components are described by the state variables velocity, piston position, pressure and the like. We collect these variables in two state vectors.

- All state variables which are given by ordinary differential equations without any constraints are collected in a vector $x \in \mathbb{R}^{n_x}$
- The vector $v \in \mathbb{R}^{n_v}$ contains velocities which are described by momentum equations with unilateral and bilateral constraints.

Summarizing the equations of all components results in the following set of equations.

Momentum equations for v

$$M\dot{v} - Wp - W_V p_V - \bar{W}^* \bar{p} = f(t, v, x) \in \mathbb{R}^{n_v} \tag{40}$$

Ordinary differential equations for x

$$\dot{x} = g(t, x, v) \in \mathbb{R}^{n_x} \tag{41}$$

Bilateral junction equations

$$W^T v + w(t) = 0 \in \mathbb{R}^{n_J} \tag{42}$$

Constraints for closed valves/orifices

$$W_V{}^T v = 0 \in \mathbb{R}^{n_{Va}} \tag{43}$$

Unilateral constraints

$$\bar{Q} \geq 0; \quad \bar{p} \geq 0; \quad \bar{Q}^T \bar{p} = 0$$
$$\text{mit} \quad \bar{Q} = \bar{W}^T v \in \mathbb{R}^{\bar{n}_a} \tag{44}$$

2.4.1. Solution

In a first step we combine the active bilateral constraint Equations (42), (43) to give

$$W_G^T v + w_G = 0. \tag{45}$$

The number of independent constraints is the rank of the matrix W_G,

$$r = \text{rank}(W_G) \tag{46}$$

The constraint equations can be fulfilled by introducing minimal coordinates

$$v_m \in \mathbb{R}^{n_{\min}} \quad \text{where } n_{\min} = n_v - r \tag{47}$$

in the form

$$v = v(v_m, t) = Jv_m + b(t). \tag{48}$$

The Jacobian J and the vector b can be calculated numerically by a singular value decomposition of the matrix W_G with the benefit that also dependent constraints can be handled. Since the column vectors of the Jacobian are orthogonal to the column vectors of W_G we can write the momentum equations as

$$J^T M (J\dot{v}_m + \dot{b}) - J^T \bar{W}^* \bar{p} = J^T f(t, x, v) \tag{49}$$

The square matrix $J^T M J \in \mathbb{R}^{n_{\min} \times n_{\min}}$ is the invertible projected mass matrix.

As a next step we derive a linear complementary problem (LCP) for the unilateral constraint equations. For this purpose we put all active unilateral constraints on a velocity level and transform Equation (44) with Equation (48) to

$$\dot{\bar{Q}} \geq 0; \quad \bar{p} \geq 0; \quad \dot{\bar{Q}}^T \bar{p} = 0$$
$$\text{where } \dot{\bar{Q}} = \bar{W}^T \dot{v} = \bar{W}^T J\dot{v}_m + \bar{W}^T \dot{b} \tag{50}$$

Together with Equation (49) we obtain

$$\dot{Q} = \underbrace{\bar{W}^T J (J^T M J)^{-1} J^T \bar{W}^*}_{A_{\text{LCP}}} \bar{p}$$
$$+ \underbrace{\bar{W}^T W^T J (J^T M J)^{-1} J^T (f - Mb) + \bar{W}^T b}_{b_{\text{LCP}}}$$
(51)

This is a standard LCP in the form

$$\dot{Q} = A_{\text{LCP}} \bar{p} + b_{\text{LCP}}$$
$$\dot{Q} \geq \mathbf{0}; \quad \bar{p} \geq \mathbf{0}; \quad \dot{Q}^T \bar{p} = 0$$
(52)

which can be solved using a standard Lemke algorithm. Experience shows that the Lemke algorithms works reliable in many cases, also for large systems, but the computing times are long. In the meantime better algorithms are available, which are based on the ideas of time-stepping and of the Augmented Lagrange method. Numerical experiences in other areas indicate, that on this new basis computing time can be shortened significantly.

With this solution of the complementarity problem the time derivative of v can be calculated. The evolution of x and v with respect to time is obtained by a numerical integration scheme, for example a Runge-Kutta-scheme.

2.4.2. Impacts

Some examples for possible impacts in hydraulic systems are:

- Valve closure
- Impacts of mechanical components, for example piston/housing contact
- Condensation of vapor (waterhammer), cavitation

In connection with the use of constraint equations instead of stiff elasticities we must consider multiple impact situations. Due to the algebraic relationship between some components sudden velocity changes in one component may cause also velocity jumps in other components. In order to calculate the velocities after an impact it is necessary to solve the impact equations for the complete system. The starting point are the momentum Equations (49). We assume as usual an infinitesimal short impact time $\Delta t \to 0$ without any position

changes. The integration of the momentum Equation (49) over the duration of the impact yields:

$$\int_t^{t+\Delta t} (J^T M J \dot{v}_m) \, dt$$
$$= \int_t^{t+\Delta t} (J^T \bar{W}^* \bar{p} + J^T f - J^T M b) \, dt$$
(53)

Denoting the beginning of the impact with $^-$ and the end with $^+$, we can rewrite Equation (53) as

$$J^T M J (v_m^+ - v_m^-) =$$
$$J^T \bar{W}^* \bar{p} \Delta t + J^T f \Delta - J^T M b \Delta t .$$
(54)

Introducing unilateral pressure impulses

$$\bar{P} = \int_t^{t+\Delta t} \bar{p} \, dt = \bar{p} \Delta t$$
(55)

and letting $\Delta t \to 0$ we come out with

$$J^T M J (v_m^+ - v_m^-) = J^T \bar{W}^* \bar{P} .$$
(56)

The unilateral constraint equations can be set up for the end of the impact in the form

$$\bar{Q}^+ \geq \mathbf{0}; \quad \bar{P} \geq \mathbf{0}; \quad \bar{P}^T \bar{Q}^+ = 0$$
$$\text{where } \bar{Q}^+ = \bar{W}^T v^+ = \bar{W}^T J v_m^+ + \bar{W}^T b ,$$
(57)

which again can be transformed into an LCP.

$$\bar{Q}^+ = \underbrace{\bar{W}^T J (J^T M J)^{-1} J^T \bar{W}^*}_{A_{\text{LCP}}} \bar{P} + \underbrace{\bar{W}^T (J v_m^- + b)}_{b_{\text{LCP}}}$$
(58)

With the solution vector $\bar{P}$ of this LCP we can calculate v_m^+ from Equation (56). Finally we get the velocity vector at the end of the impact as $v^+ = J v_m^+ + b$.

3. Example

As an example from industry we consider the hydraulic safety brake system of a fun ride, the free fall tower [1]. It is manufactured by the company Maurer Söhne GmbH, Munich, Germany. Figure 12 shows the tower. Under normal operation conditions the cabin with the passengers is lifted by a cable winch to a height of about

Fig. 12 Free fall tower

60 m. Subsequently the cabin is released and falls down nearly undamped. Before reaching the ground the normal brake system stops the cabin softly via the cable winch. For safety reasons a redundant brake system is

necessary. In the case of a failure of the normal operating brake or a cable rupture the safety brake system has to catch the cabin even under disadvantageous conditions.

The safety brake system is a hydraulic system which moves brake-blocks via hydraulic cylinders. For this purpose steel blades are fixed at the cabin. The steel blades fall into a guide rail, where the brake-blocks are fixed. The safety brake system consists of up to 7 identical modules with 4 hydraulic cylinders each. The modules are arranged upon each other. Figure 13 shows the model of the system. The simulations were carried out with the computer programme *HYSIM*. As the Fig. indicates, the programme *HYSIM* allows multi-hierarchical modelling of systems. It means that some components can be put together to form a group, which itself can be used and duplicated like any elementary component.

Under normal operating conditions the brake-blocks are moved outwards the guide rail quickly so that the system is decelerated softly by the winch. Only under bad conditions the safety brakes stay closed and the cabin will be stopped by the friction forces. Due to the very short opening time of the brake the hydraulic cylinders move quickly and reach the stop position with high velocities. The resulting impact forces caused in some cases damage of the cylinders. In order to reduce the impact forces simulations were carried out. The aim was to find new values of adjustable parameters such that the impact velocities are reduced and the opening time does not exceed a certain maximum value.

Figure 14 shows some simulation results. The impact velocity and thus the resulting force is significantly high for the Cylinder 1. The reason for this behavior lies in the different length of the supply line and the different movement direction (up/down) of the cylinders, i.e. hydraulic and mechanical asymmetries. The impact velocities can be reduced significantly by increasing restriction parameters at some valves, as Fig. 14 shows. This simple measure has been adopted to the real system and no problems occurred since then.

A comparison of measurement and simulation is given in Fig. 15. As the cylinders start moving the pressure increases due to the increasing spring force of the cylinders. At $t \approx 0, 37s$ the last cylinders reaches the stop position. The impact causes a pressure jump.

The model for the drop tower consists of nearly 1000 hydraulic degrees of freedom, computing time was in the range of less than one hour. A comparison of the computing time with that of convential and commercial

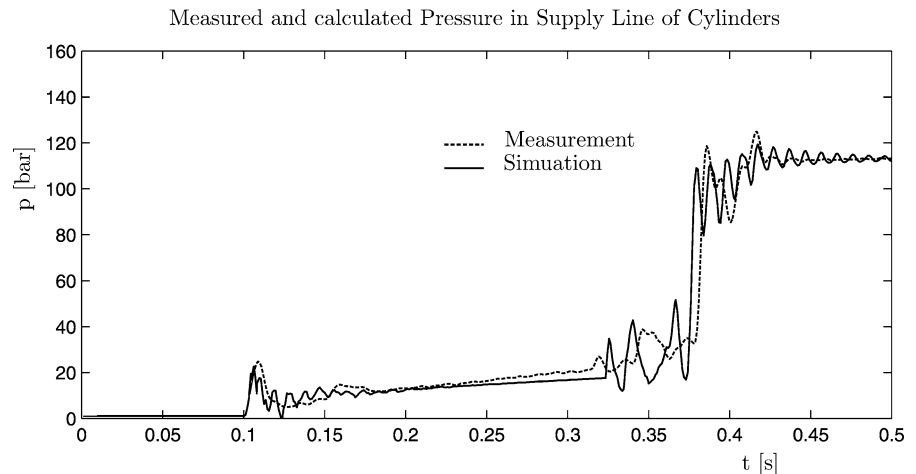**Fig. 13** HYSIM-model of the hydraulic system
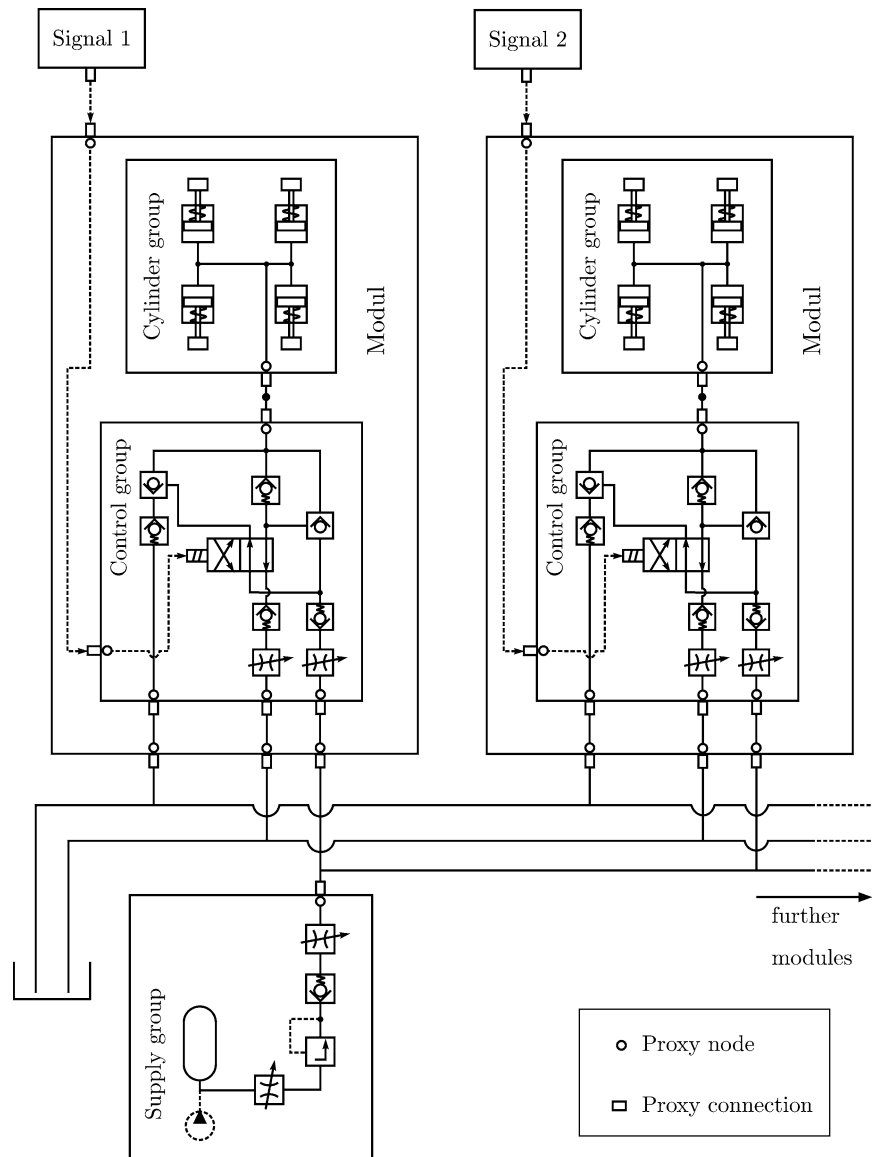
codes results in a factor of about 6000 to 10000. This large difference for the new model has been also confirmed by many other problems from industry.

4. Summary

The theories of non-smooth mechanics include measure differential equations, differential inclusions and complementarities, the first ones to regard in an elegant way unsteady events like impacts, the second ones to describe set-valued force laws, which appear in many applications least in an approximate way. Force laws with very steep characteristics are typical

in many technical areas like mechanics, fluid mechanics or electronics. As in many cases the evaluation of the dynamical behavior of such systems is really cumbersome and time-consuming, the idea of deregularizing such systems makes sense. It is applied to hydraulic systems, which are usually represented by classical approaches leading to very large computing times. The above idea results in a completely new description with a better performance.

As has been shown in some detail, the basic key is to replace stiff differential equations by non-stiff ones including bilateral and unilateral constraints, the last ones in connection with complementarities. Ex-

Fig. 14 Cylinder
movement

Velocity Cylinder 1

Velocity Cylinder 2

Velocity Cylinder 3

Velocity Cylinder 4
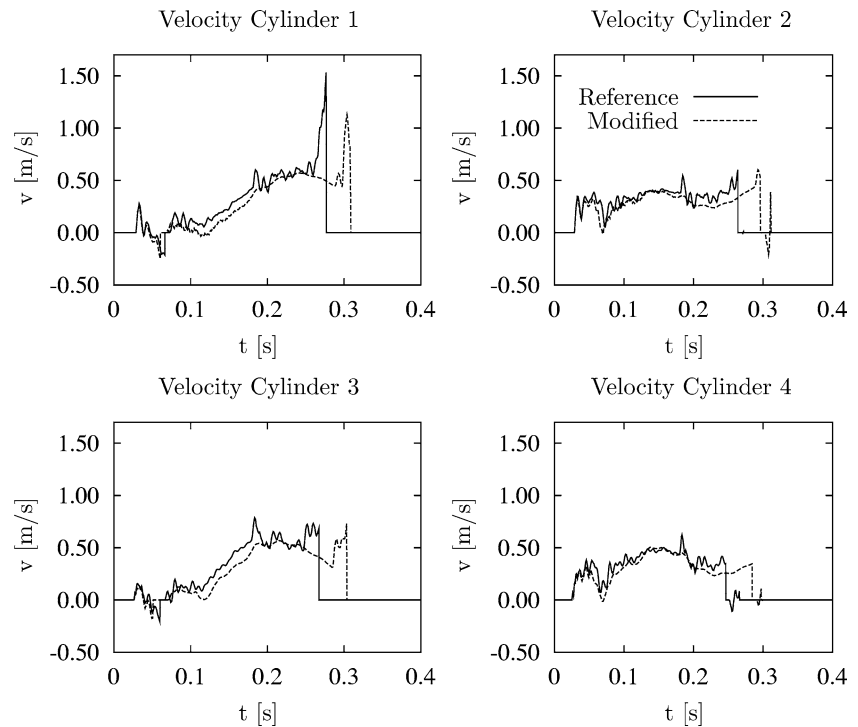
Fig. 15 Comparison
measurement/simulation

Measured and calculated Pressure in Supply Line of Cylinders

amples of basic components with stiff behavior are given together with their algebraic substitutes. The resulting equations possess a strong structural similarity with those of mechanical multibody systems. It is a set of nonlinear ordinary differential equations with unilateral and bilateral constraints in the form of equality and inequality constraints. The bilateral constraints can be eliminated by certain Jacobians being evaluated numerically. The unilateral constraints accompanied by a linear complementarity problem (LCP) are solved by a classical Lemke's algorithm, in future by an Augmented Lagrange method. The numerical pro-

cesses are laid down in a large computer code HYSIM, which allows to consider any configurations of large hydraulic systems. An example from industry is presented.

References

1. Borchsenius, F.: Simulation ölhydraulischer systeme, Fortschrittberichte VDI, Reihe 8, Nr. 1005, VDI-Verlag, Düsseldorf, (2003)
2. Brommundt, E.: Ein Reibschwinger mit selbsterregung ohne fallende reibkennlinie. ZAMM, angew. Math. Mech. **75**, 811–820 (1995)

3. Foerg, M., Pfeiffer, F., Ulbrich, H.: Simulation of granular media by rigid body dynamics. In: Proceedings of ECCOMAS Thematic Conferences on Advances in Computational Multibody Dynamics, Lisbon (2003)
4. Glocker, Chr.: Set-Valued Force Laws. Springer, Berlin, Heidelberg, New York (2001)
5. Leine, R.I., Nijmeijer, H.: Dynamics and Bifurcations of Non-smooth Mechanical Systems. Springer, Berlin, Heidelberg, New York (2004)
6. Moreau, J.J., Panagiotopoulos, P.: Topics in Non-smooth Mechanics. Birkhäuser, Basel (1988)
7. Pfeiffer, F.: Unilateral Problems of Dynamics. Archive of Applied Mechanics. Springer, Berlin, pp. 503–527 (1999)
8. Pfeiffer, F., Glocker, Chr.: Multibody Dynamics with Unilateral Contacts. Wiley, New York (1996)
9. Pfeiffer, F., Borchsenius, F.: New hydraulic system modeling. J. Vib. Control **10**, 1493–1515 (2004)